Satellite Attitude Acquisition by Momentum Transfer

Peter M. Barba*
Aeronutronic Ford Corporation, Palo Alto, Calif.
and
Jean N. Aubrun†
Lockheed Missles and Space Company, Palo Alto, Calif.

Transition between spin-stabilized orbit injection and three-axis control mode may be achieved by simple momentum transfer from the satellite to a momentum wheel. This open-loop process provides both despin and spacecraft reorientation. A time simulation of the maneuver, illustrated by means of a computer-animated motion picture, reveals an extremely complex motion. However, key features may be explained in a quasistatic fashion using geometrical interpretation of energy and momentum laws. An evolution equation is presented to help design wheel-torquing strategies.

Nomenclature

B	= rigid body
$\bar{B}_1, \bar{B}_2, \bar{B}_3$	= unit vectors parallel to principal axes of B
C	= composite rigid body
E_C	= kinetic energy of C
EE	= energy ellipsoid
$\bar{H}$	= system angular momentum
$\bar{H}_C$	= angular momentum of C
$\bar{H}_W$	= angular momentum of W
h	= magnitude of $\bar{H}_W$ (angular momentum of wheel W)
I_1, I_2, I_3	= moment of inertia components of system with respect to principal axes of C
$\bar{L}$	= torque acting on B
MS	= momentum sphere
P	= tip of the angular momentum vector on MS
T	= motor torque
$\bar{\omega}$	= angular velocity vector
ω_s	= angular velocity of the system
θ	= angle between $\bar{H}$ and $\bar{B}_2$
$\bar{u}$	= unit vector parallel to momentum wheel axis
W	= momentum wheel

Introduction

MANY current satellites, which are three-axis controlled on orbit, are spin-stabilized during ascent and orbit injection. Recent work has shown that a convenient transition between the two control modes may be achieved by transferring angular momentum from the spinning spacecraft to a momentum wheel that is initially orthogonal to the system momentum vector.‡ The procedure, which can be carried out in an open-loop manner, simultaneously achieves both final despin and satellite reorientation to the nominal three-axis attitude. A similar procedure applies to the recovery of dual-spin satellites from a so-called flat-spin condition.

Though based upon a simple principle, the actual vehicle motion is difficult to grasp. It is governed by nonlinear equations for which no general closed-form solution is available. An elegant perturbation analysis has been made by Gebman,[1] but a large fraction of the design studies still rests upon digital simulation, the results of which are often difficult to interpret or extrapolate. Two original contributions to the solution of this problem are presented here to help in visualizing the actual maneuver and to provide a deeper analytical insight into its dynamics.

First, a mathematical description of the system makes it possible to deduce the key features of this process and, eventually, to explain some unexpected results encountered in simulations. It is based upon a geometrical interpretation of the energy and momentum laws. The various properties of the motion are shown to be dependent upon the way the "momentum sphere" and the "energy ellipsoid" intersect each other. This method uses a quasistatic approach which easily can predict the stability of the system with or without energy dissipation. The effect of the inertial properties of the system (direction of principal axes vs wheel axis) upon the residual error angle is obtained from limit properties of these surfaces. The evolution of the system is shown to be ruled by the scalar product of two vectors (the wheel torque and the vehicle angular velocity) which easily can be constructed geometrically. This approach suggests that, in addition to the simple constant-torque acquisition, various optimal or closed-loop wheel-torquing strategies could be derived to improve the maneuver in terms of acquisition time, final attitude errors, etc.

Second, an animated motion picture, which has been generated entirely by a digital computer, accurately depicts the satellite motion during the various phases of the transition, from the time simulation to the three-dimensional drawings of a simplified satellite. Hidden line techniques have been used to improve depth perception and several key parameters have been plotted simultaneously during the sequence.

Basic Principles

Consider a gyrostat satellite (represented in Fig. 1) as a wheel W contained in a rigid body B. $\bar{B}_1, \bar{B}_2$, and $\bar{B}_3$ are unit vectors aligned with centroidal principal axes of B. Wheel W rotates about an axis $\bar{u}$ fixed in B parallel to $\bar{B}_2$. The angular velocity of B relative to inertial space is expressed in body components as

$$\bar{\omega} = \omega_1 \bar{B}_1 + \omega_2 \bar{B}_2 + \omega_3 \bar{B}_3$$

Conservation of angular momentum states that the system angular momentum $\bar{H}$ will remain constant in inertial space in the absence of external torques. This brings to mind two possible motions for the system. One is illustrated in Fig. 1 where W is stationary with respect to B, and $\omega_1 = \omega_2 = 0$, $\omega_s = |\bar{H}|/I_3$. $\bar{B}_3$ is thus parallel to $\bar{H}$. The other motion,

Received Sept. 12, 1975; revision received Jan. 20, 1976.
Index category: Spacecraft Attitude Dynamics and Control.
*Principal Engineer, WDL Division.
†Research Scientist, Palo Alto Research Laboratory.
‡This technique has been developed as an IR&D project by the Aeronutronic Ford Corporation and will be the subject of a patent application.

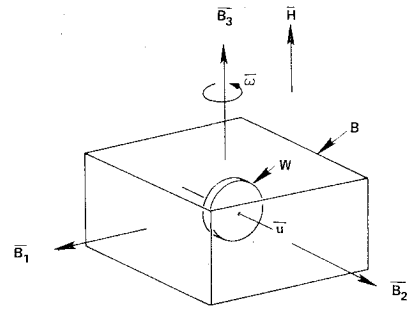

Fig. 1 Initial satellite configuration, $\omega = \omega_S B_3$, $\omega_{W/B} = 0$.

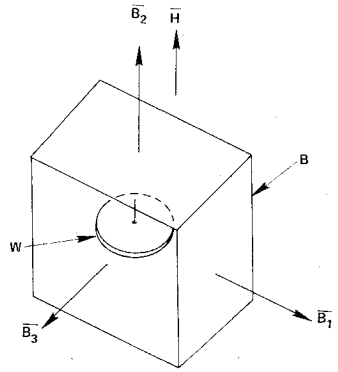

Fig. 2 Final configuration, $\bar{\omega} = 0$, $\bar{\omega}_{W/B} \neq 0$.

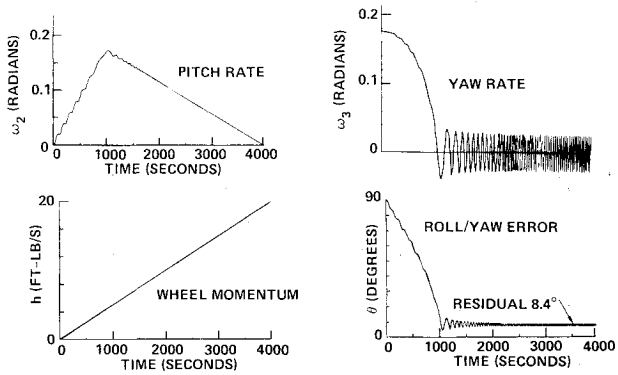

$I_1 = 86.24$, $I_2 = 85.07$, $I_3 = 113.59$ slug-ft^2

$\omega_1(0) = \omega_2(0) = 0$, $\omega_3(0) = 0.1761$ rad/s, $T = 0.005$ ft-lb

Fig. 3 Computer simulation results for momentum transfer maneuver.

illustrated in Fig. 2, shows $\bar{\omega} = 0$; W is rotating so that the entire system angular momentum is stored in W, and $\bar{B}_2$ is then parallel to $\bar{H}$.

The attitude acquisition scheme, then, is to start with the spinning configuration of Fig. 1, energize a motor to spin W relative to B, which transfers momentum from B to W, thus arriving at the configuration shown in Fig. 2. The body motion is rather complex and may be found by numerical integration of the differential equations governing the motion of such a gyrostat. The equations used for the simulation consist of the Euler dynamic equations developed herein as Eq. (8). The results of such a simulation are shown in Fig. 3. A constant motor torque T causes a linear increase in h, the component of the inertial angular momentum of W parallel to $\bar{u}$. The inertial spin rate ω_3 decreases and the cross-axis rate ω_2 increases to a peak as the momentum is transferred from the 3 axis, and then decreases as the momentum is transferred to the wheel. The angle θ between $\bar{H}$ and $\bar{B}_2$ starts at 90° and decreases to a low value. This simulation illustrates that the maneuver does not proceed as planned. ω_2 and θ do not

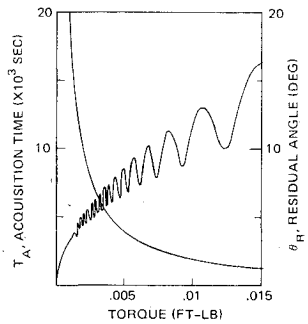

Fig. 4 Residual angle and acquisition time vs torque.

decrease to zero as desired. In fact, it can be shown by repeated simulations that the residual angle θ is a function of (increases with) the magnitude of T as seen in Fig. 4. The acquisition time decreases since the rate of change of h is proportional to T, the motor torque. To provide a fuller understanding of the maneuver, the computer simulation results were used to generate a motion picture (Fig. 5 contains representative frames).

Momentum and Energy Surfaces

The system total angular momentum $\bar{H}$ is constant in inertial space. In body coordinates, its orientation may change, but its length H remains constant. Thus, the extremitiy P of $\bar{H}$ lies on a sphere, the "momentum sphere" (MS).

It is convenient at this point to introduce the concept of a composite rigid body C that is fixed with respect to body B and in which the inertia dyadic includes the body B inertia dyadic plus the dyadic of the wheel, where the moment of inertia along the axis u is taken to be zero. This amounts to lumping into the body C all the inertia contributions that do not involve the wheel rotation. Thus, the system equivalently is modeled by a rigid body C and a wheel W that possesses a moment of inertia only along its spin axis.

The kinetic state of the system is defined completely by the wheel momentum, $\bar{H}_W = h\bar{u}$, and the representative point P on MS (the direction of $\bar{H}_W$ is fixed in B). At each instant the body angular momentum $\bar{H}_C$ is such that

$$\bar{H}_C + \bar{H}_W = \bar{H} \tag{1}$$

From this simple equation it seems that by increasing the magnitude of $\bar{H}_W$, $\bar{H}_C$ should decrease, so that Eq. (1) could be maintained. $\bar{H}_C$ eventually will vanish when $\bar{H}_W = \bar{H}$. However, since Eq. (1) is a vector equation, and the only controlled variable is the length of $\bar{H}_W$, a closer examination of the process is needed. Consequently, another important quantity is considered, the kinetic energy E_C of the composite body C. This is expressed classically as

$$E_C = \frac{1}{2}\bar{H}_C \cdot \bar{\omega} = \frac{1}{2}\sum_{i=1}^{3} H_{C_i}^2 / I_i$$

where I_i represents the principal inertias of the composite body C, and H_{C_i} represents the components of $\bar{H}_C$. Making use of Eq. (1), we have, with obvious notation,

$$E_C = \frac{1}{2}\left[\frac{(H_1 - H_{W1})^2}{I_1} + \frac{(H_2 - H_{W2})^2}{I_2} + \frac{(H_3 - H_{W3})^2}{I_3}\right] \tag{2}$$

Thus, for a given body kinetic energy E_C, and a given wheel momentum $\bar{H}_W$, Eq. (2) shows that P lies on the energy ellipsoid (EE). The axes of EE are parallel to the principal axes of the system, but its center is displaced from the origin by the

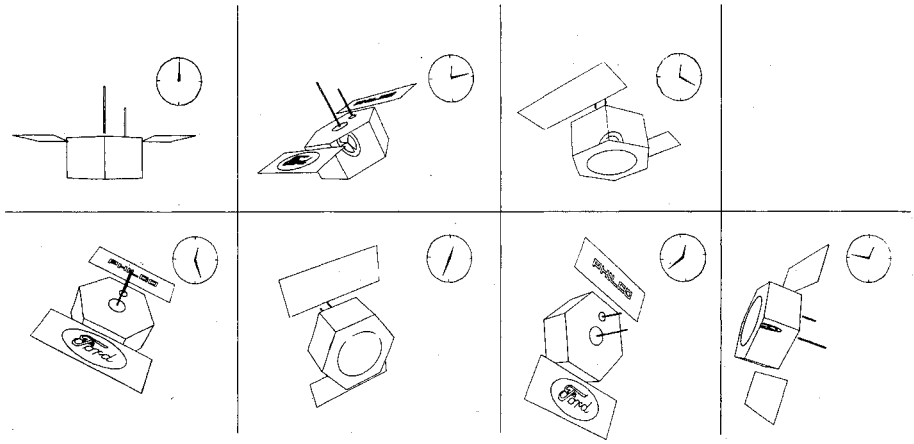

Fig. 5 Frames from motion picture illustrating simulation results.

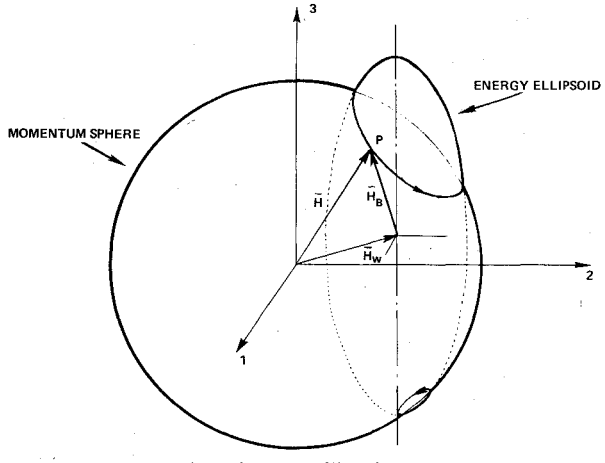

Fig. 6 Intersection of energy ellipsoid and energy spheres.

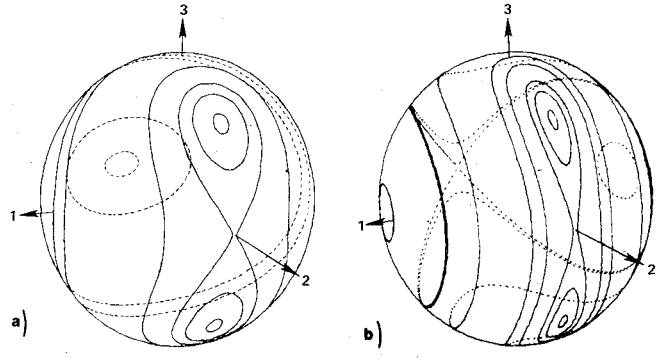

Fig. 7 Energy levels shown on momentum sphere: a) $I_3 > I_1 > I_2$; b) $I_3 > I_2 > I_1$.

vector $\bar{H}_W$. The semimajor axes of this ellipsoid are proportional to the square root of the corresponding inertia. Thus, the energy ellipsoid is not to be confused with the more classical "inertia" or "momentum" ellipsoids which are, in a sense, reciprocals of *EE*.

Now, if the wheel momentum is constant (no torque applied to the wheel), to satisfy both energy and momentum equations the point *P* must lie at the intersection of *MS* and *EE*. This intersection is a closed, simply connected curve and it is convenient to trace it on *MS*. As time varies, this curve is described by *P* in a direction prescribed by Euler's equations of motion; therefore, it can be thought of as an "orbit" associated with a given energy level (Fig. 6). By tracing a set of curves corresponding to different values of E_C, an energy mapping is obtained on *MS* as shown in Fig. 7.

Stability of the System

An immediate and useful application of these orbits is the derivation of stability criteria from their shape and the evolution of their shape.

Stability at the Origin

First, if the body cannot dissipate energy at all, the "stability at the origin" (in the Liapunov sense) is deduced directly from the shape of the orbits in the neighborhood of the point under consideration. The system will be declared stable if *P* will stay in the neighborhood of its initial position. Obviously, the shape of the orbits depends upon the size of *EE* (the value of the energy), its relative shape (the relative magnitude of the inertias), and its position (the value of the wheel momentum). For instance, Fig. 7a shows different intersections corresponding to different values of E_C. The inertias for this example are in the order $I_3 > I_1 > I_2$.

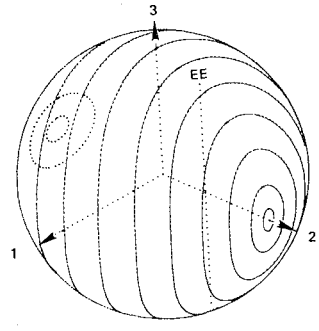

Fig. 8 Energy levels on momentum sphere with increased wheel momentum $\bar{H}_W$.

The analog of the "separatrix" of the Poinsot representation appears here also, and clearly two stable points are in the 2-3 plane (the two "eyes") and another one on the negative side of the 2 axis. For the case of Fig. 7b ($I_3 > I_2 > I_1$), the two stable points are still there, but the third one is replaced by two symmetric points on the 1 axis.

These results are unusual in that they depart from the usual result that an intermediate axis is always unstable. The reason for this behavior is that the shift of *EE* because of the wheel momentum causes a shift in the separatrices pattern, thus appearing as if this momentum effectively had increased the inertia on the 2 axis.

As $\bar{H}_W$ is increased, one side of *EE* is pushed out of *MS* and the orbit always encloses the 2 axis, no matter what the values of I_1 and I_2 (Fig. 8). Of course, when $\bar{H}_W = 0$, the classical results are obtained as with the Poinsot theory, but the advantages of using the *MS-EE* description are threefold: 1) the curves are traced on a sphere, which is easier to handle than an ellipsoid; 2) the existence of stored momentum in the system can be described easily; and 3) the energy dissipation case, which is most useful in practical application, follows quite naturally.

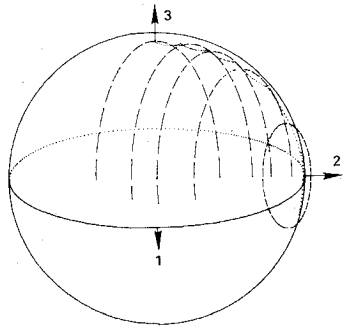

Fig. 9 Quasistatic distribution of maneuver showing successive energy states.

Asymptotic Stability

The stability problem is quite different when the body is able to dissipate energy. Whether part of it is transmitted to the wheel or in some other internal device does not matter in this analysis. The question is, what happens when the energy decreases? In this case, the size of *EE* diminishes with time, and one then must observe the corresponding deformation of the orbits. Asymptotic stability (in the Liapunov sense) means that the orbit surrounding a point *P* must become smaller when *EE* shrinks, eventually tending asymptotically to a single point at *P*. There is indeed a minimum size of *EE*, which corresponds to *EE* and *MS* being tangent with *EE* inside. There is also a maximum size if *MS* is inside, since *EE* and *MS* must always have at least one common point. From Fig. 7 it can be seen that the two eyes are the only asymptotically stable points. In the case of Fig. 8, the point of the 2 axis is stable.

From this analysis it is concluded that energy dissipation will be a stabilizing factor in this maneuver. Of course, it should be noted that these results are only valid if the dissipating mechanism does not create a change in the inertias that significantly distorts these energy maps. In the present case, however, once a point close to the 2 axis has been reached, and if the energy is decreasing, there is no possibility other than staying on this axis.

Quasistatic Description of the Maneuver

At the beginning of the acquisition maneuver, the motion is a simple spin about the 3 axis (the axis of maximum inertia) and the wheel is at rest. *EE* is thus tangent to *MS* at two symmetric points on the 3 axis. A constant torque T is then applied to the wheel, whose momentum h increases linearly with time at the expense of the body momentum, thus causing the point *P* to move toward the 2 axis.

The motion of this system can be best understood as a succession of equilibrium states where the point *P* goes from one orbit to the next as *EE* is shifted away from the 3 axis because of the increase in wheel momentum (Fig. 9). As long as these successive orbits remain of small radius, *P* will remain close to the 2-3 plane; and by the time it reaches the 2 axis, the residual error will be small. It can be seen intuitively that, if the torque applied to the wheel is small enough, *EE* will stay almost tangent to *MS* and the corresponding orbits will remain small. Conversely, if the wheel momentum is increased abruptly (i.e., in a time smaller than the energy relaxation time), then *EE* will be pushed out of *MS* without changing size, thus increasing the size of the orbit.

Although this geometrical construction is applicable to an arbitrarily oriented wheel, by assuming that $\bar{H}_W$ is on the 2 axis, important features of this motion readily may be deduced. There is a critical value for h beyond which the orbits are always about the 2 axis for any value of the energy. By pure geometrical consideration (shown in the Appendix), this value is given by

$$h_0 = H(I_3 - I_2)/I_3$$

This defines a critical time t_0 such that

$$t_0 = (I_3 - I_2)\omega_s / T \qquad (3)$$

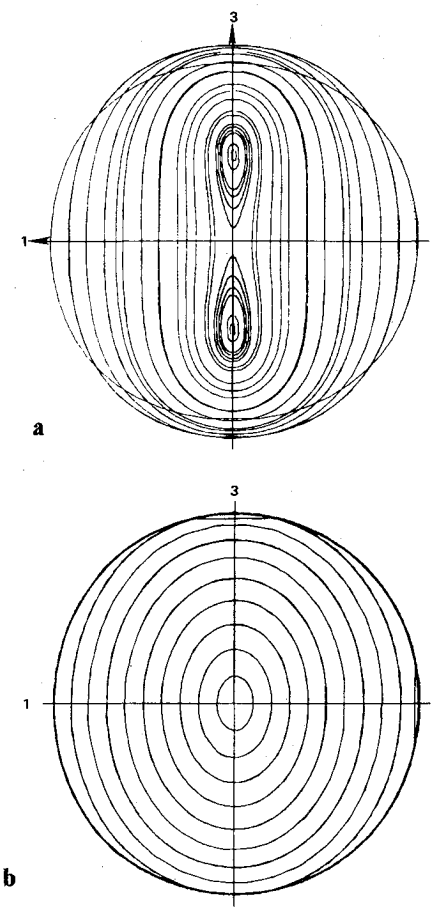

Fig. 10 Orbits projected on 1-3 plane: a) $t < t_0$; b) $t > t_0$.

where ω_s is the initial spin rate about the 3 axis. This t_0 is the time at which the angle between the momentum $\bar{H}$ and the 2 axis is close to zero, and beyond which the orbits are always circling about this 2 axis. Thus, if the orbit size is small at that time, so will be this angle, which is the acquisition error angle; and from our previous inference, the smaller the torque, the smaller the error.

This qualitative result indeed was found quantitatively in the computer simulations as depicted by Fig. 4. The periodic behavior exhibited in this example is quite typical and is due to a "phasing" phenomenon. Depending on the exact time at which the jump is made from the last orbit circling an axis parallel to the 3 axis (this time being, of course, in the vicinity of t_0), different final orbits may be reached; thus the results of Fig. 4. This may be seen more clearly in Fig. 10, where the system of orbits is projected on the 1-3 plane before and after t_0.

The positions of the eyes in Fig. 10a are related to the wheel momentum and move toward the origin as h increases. At some point, the topology changes to that of Fig. 10b. The point where the transition is made determines the size of the last orbit; thus the residual error.

After the transition at t_0, time is spent despinning the satellite about the 2 axis, since H_C is now close to that axis. When H_{C_2} is zero, $h = H$, and *EE* has its center on *MS*. This occurs at a time

$$t_A = I_3 \omega_s / T \qquad (4)$$

It is only then that the maneuver is really completed. This acquisition time t_A was also plotted on Fig. 4.

System's Evolution: Torquing Strategies

The quasistatic approach is useful in understanding the principal features of the motion and the stability of the

system. To go even further, a powerful evolution equation is to be considered, which expresses the rate of change of energy as

$$dE_C/dt = -\bar{L}\cdot\bar{\omega} \tag{5}$$

where $\bar{L}$ is the torque acting on the body. Since the same torque applies to the wheel, $d\bar{H}_W/dt = -\bar{L}$. This $\bar{L}$ contains the reaction torques as well. However, taking the time derivative in body coordinates, we have

$$\bar{L} = -d\bar{H}_W/dt = -\dot{\bar{H}}\omega - \bar{\omega}\times\bar{H}_W$$

and Eq. (5) becomes simply

$$\dot{E} = dE_C/dt = -\dot{h}(\bar{\omega}\cdot\bar{u}) \tag{6}$$

For the case where $\bar{u}$ is on the 2 axis,

$$\dot{E} = -T\omega_2 \tag{7}$$

The Euler equations of motion are then

$$I_1\dot{\omega}_1 = (I_2 - I_3)\omega_2\omega_3 + h\omega_3 \tag{8a}$$

$$I_2\dot{\omega}_2 = (I_3 - I_1)\omega_1\omega_3 - T \tag{8b}$$

$$I_3\dot{\omega}_3 = (I_1 - I_2)\omega_1\omega_2 - h\omega_1 \tag{8c}$$

$$\dot{h} = T \tag{8d}$$

When T is small enough, and $t \le t_0$, a first-order solution using an asymptotic expansion with smallness parameter $T/(I_3\omega_s^2)$ is

$$\omega_2 = [T/(I_3 - I_2)]\,[t - (I_3/\omega_n I_2)\sin\omega_n t] \tag{9}$$

where

$$\omega_n = \omega_s\{[(I_3 - I_2)(I_3 - I_1)]/I_1 I_2\}^{1/2}$$

Integrating Eq. (7) with Eq. (9) leads to

$$E = \frac{1}{2} I_3\omega_s^2 - \frac{T^2t^2}{2(I_3 - I_2)} + \frac{I_3T^2}{I_2(I_3 - I_2)\omega_n^2} \times (1 - \cos\omega_n t) \tag{10}$$

or, since $h = Tt$,

$$E = E_0 - \frac{h^2}{2(I_3 - I_2)} + \frac{I_3T^2}{I_2(I_3 - I_2)\omega_n^2} \times (1 - \cos\omega_n t)$$

Now again, by solving algebraically the intersection of EE and MS, it can be shown that the condition for EE to be tangent to MS is that the energy be

$$E_m = E_0 - h^2/[2(I_3 - I_2)]$$

Thus Eq. (10) may be written as $E = E_m + \Delta E$; and it becomes obvious that the less the torque, the less ΔE, and thus the smallest orbit radius (and hence residual angle), since EE will be almost tangent to MS.

An interesting control possibility is to design open-loop sequences other than constant torque sequences from 0 to t_A. By using energy-orbit mapping, it is possible to make discrete jumps in wheel momentum and go from one orbit to another directly. This technique may be appealing if low torques are difficult to obtain with existing wheels; large torques for short timing periods then will be more appropriate. In this case, of course, precise timing is important and precise knowledge of the system inertias also is required.

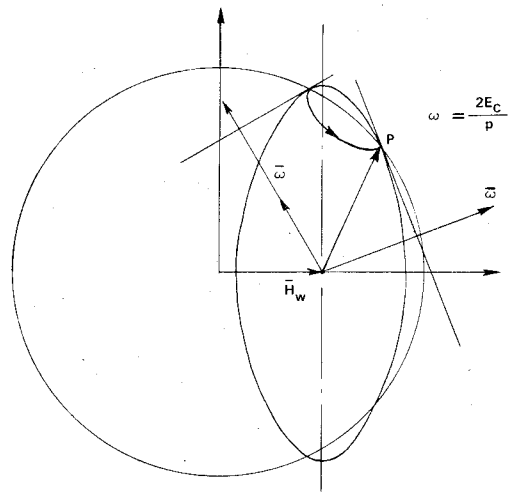

Fig. 11 Construction showing calculation of angular velocity magnitude ω.

The energy ellipsoid has another property: the direction and magnitude of the vector $\bar{\omega}$ may be obtained directly from EE by the construction shown in Fig. 11. If p is the distance from the center of EE to the tangent plane of the point P, the magnitude of ω is $\omega = 2E_C/p$, and its direction is perpendicular to this tangent plane.

Summary

The attitude acquisition maneuver treated here is the same problem as recovery of a dual-spin satellite from a flat spin. Visualization of the complex motions of this momentum exchange maneuver is aided by use of a quasistatic momentum sphere-energy ellipsoid concept. Indeed, this geometric approach to understanding the motion yields analytical results and leads to possible control law strategies for attitude acquisitions. Computer-generated motion pictures also have proven to be useful tools, aiding in the visualization of the maneuver.

Appendix: Derivation of the Critical Time t_0

The difference between the patterns shown in Figs. 10a and 10b can be determined by considering the intersection of the EE and the MS in the 2-3 plane, i.e., the intersection of the circle and the ellipse whose equations are, respectively,

$$H_2^2 + H_3^2 = H^2$$

$$(H_2 - h)^2/I_2 + H_3^2/I_3 = 2E_C$$

In general, these equations have two roots, and this corresponds to the case of Fig. 10a. The general solution for H_2 is

$$H_2 = I_3h/(I_3 - I_2) \pm \Delta^{1/2}$$

where Δ is a function of h and E_C. However, H_2 is a valid solution only if it is less than H. Thus, if h is such that $I_3h/(I_3 - I_2) > H$, then there is at most one solution for H_2, and this is the case of Fig. 10b. This means that if the wheel momentum is larger than

$$h_0 = [(I_3 - I_2)/I_3]H$$

the orbit will always be around the 2 axis, no matter what the energy (Figs. 8 and 10b). Since h is related to the torque by $h = Tt$, for any time

$$t > t_0 = [(I_3 - I_2)\omega_s]/T$$

it is guaranteed that the orbit will always be about the 2 axis.

Reference

[1] Gebman, J. R. and Mingori, D. L., "Perturbation Solution for the Flat Spin Recovery of a Dual-Spin Spacecraft," *AIAA Journal*, Vol. 14, July 1976, pp. 859-867.